Supporting Information

Microbe-engaged synthesis of carbon dots-decorated reduced graphene oxide as high-performance oxygen reduction catalysts

Lihua Zhou[a], Peng Fu[a], Yueqiang Wang[b], Lihua Sun[a], Yong Yuan[b,*]

[a] School of Chemical Engineering and Light Industry, Guangdong University of Technology, Guangzhou 510006, China

[b] Guangdong Key Laboratory of Agricultural Environment Pollution Integrated Control, Guangdong Institute of Eco-Environmental and Soil Sciences, Guangzhou 510650, China

Table S1 Chemical compositions of the graphene-based materials and the CDs-derived from *S. oneidensis*

Samples	C%	O%	N%	P%	S%
C-rGO	86.4	12.9	--	--	--
M-rGO	83.2	11.8	3.9	0.3	0.6
CDs/M-rGO	71.8	15.4	11.6	0.3	0.8
CDs	62.8	20.8	13.1	0.3	1.0

-- Undetectable

Table S2 Summary of reported ORR performance of carbon nanomaterials-graphene hybrids and bacteria-derived carbon materials in 0.1 M KOH.

Catalyst	Precursor	Treatment	Onset potential (V vs. RHE)	Reference
N-CDs/G	*Coal-based rod*	Electrochemical etching	0.82[a]	Chem. Commun. 2015, 51, 3419.
GQD-GNR	Na+hyxabromobenzene +methylbenzene	Hydrothermal+annealing at 1000 °C	0.94[a]	J. Am. Chem. Soc. 2015, 137, 7588.
BN-GQD/G	Graphite and anthracite	Hydrothermal+annealing at 1000 °C in the presence of boric acid and NH_3 gas	0.96	ACS *Nano 2014,* 8, 10837-10843
N,S-RGO/GQDs	Graphite and glutatione	Treated at 200 °C under microwave irradiation	0.86	J. Mater. Chem. A 2014, 2, 20605.
Carbonaceous rGO/E. coli composite	Graphene+Bacteria	Annealing at 900 °C	0.87	J. Mater. Chem. A 2015, 3, 12873.
HQDC-1000	Shewanella bacteria	Annealing at 900 °C	0.91	Sci. Rep. 2015, 5, 17064.
BZ-800	*Bacillus* bacteria	Annealing at 800 °C in the presence of $ZnCl_2$	0.90	Adv. Funct. Mater. 2013, 23, 1305.
CDs/M-rGO	**Graphite and *Shewanella* bacteria**	**Microbial reduction and hydrothermal treatment at 180 °C**	**0.94**	**This work**

[a] Estimated from the LSV curves in the references

The potentials were converted with the equations:

$E_{RHE} = E_{SCE} + 0.2438\ V + 0.0591 \times pH$

$E_{RHE} = E_{Ag/AgCl} + 0.197\ V + 0.0591 \times pH$

Figure S1

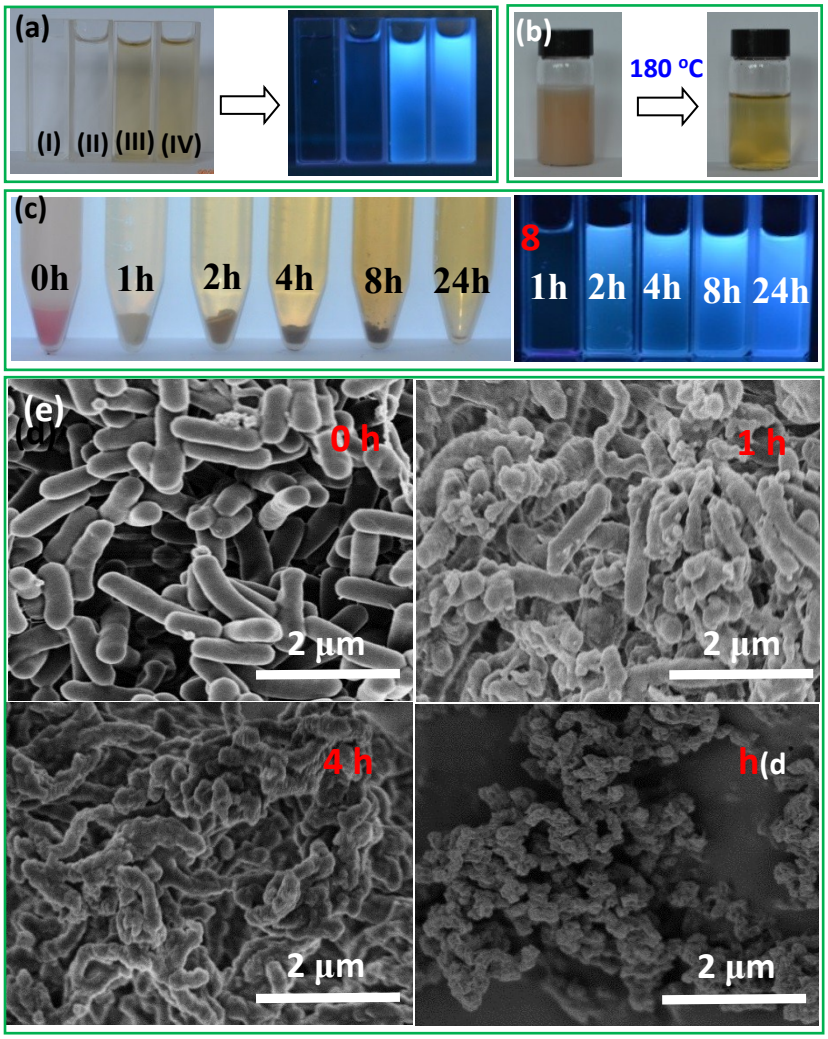

Figure S1 (a) Photographs of the supernatants of the hydrothermally treated C-rGO (I), M-rGO (II), *S. oneidensis* (III), and the mixture of M-rGO and bacterial cells (IV) under illumination of white light and UV(365 nm) light; (b) Photographs of *S. oneidensis* suspension before and after hydrothermal treatment for 24 h at 180 °C; (c) Photographs of hydrothermally treated *S. oneidensis* sampled at different time intervals, and (d) the corresponding supernatants under illumination of UV(365 nm) light; (e) SEM images of the pellets sampled at different time intervals, which show the gradually degradation of bacterial cells during the hydrothermal treatment.

Figure S2

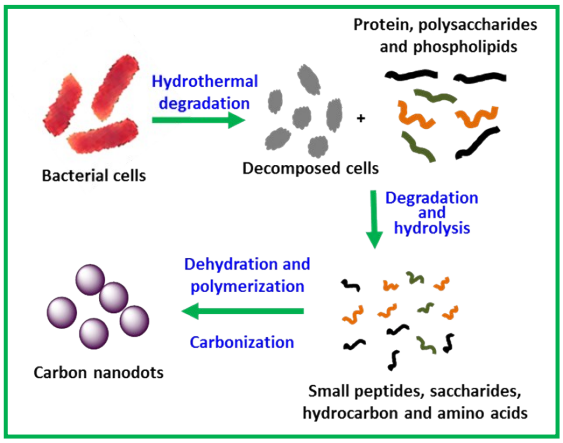

Figure S2 Schematic illustration of the formation mechanism of the CDs from bacterial cells.

Figure S3

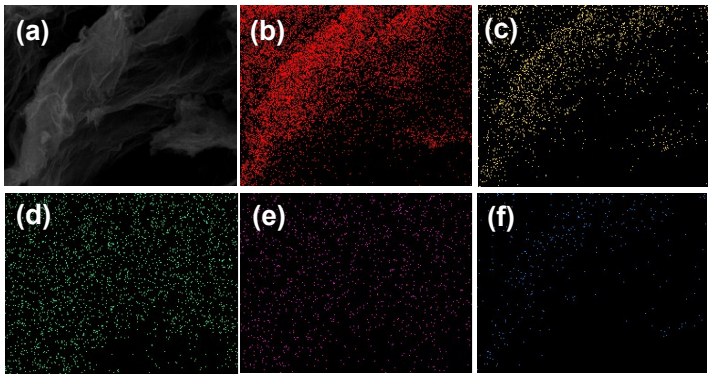

Figure S3 SEM image of the M-rGO (a) and corresponding quantitative EDS element mapping of C (b), O (c), N (d), S (e) and P(f).

Figure S4

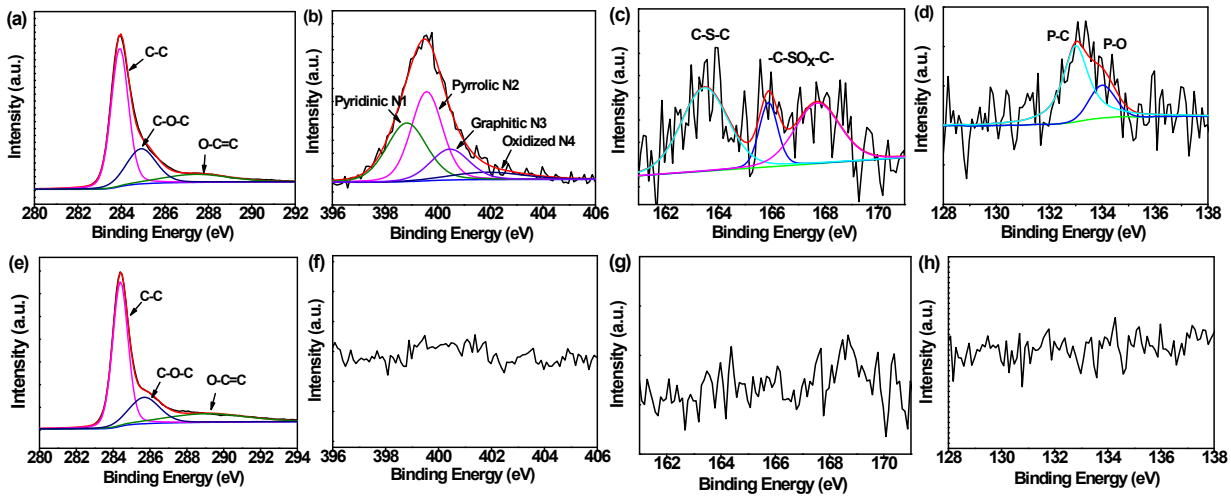

Figure S4 High resolution C 1s (a), N 1 s (b), S 2p (c), and P 2p (d) XPS scans of the M-rGO; High resolution C 1s (e), N 1 s (f), S 2p (g), and P 2p (h) XPS scans of the C-rGO.

Figure S5

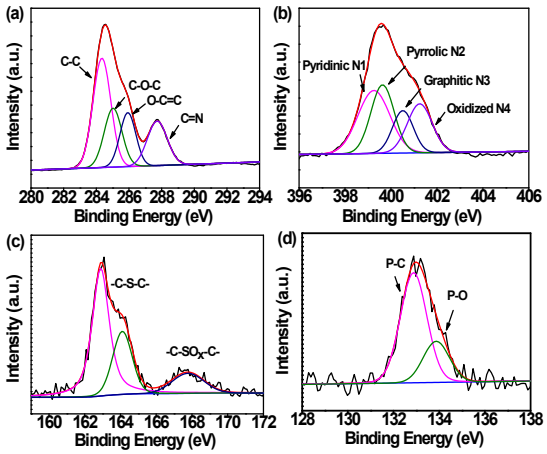

Figure S5 High resolution C 1s (a), N 1 s (b), S 2p (c), and P 2p (d) XPS scans of the *S. oneidensis*-derived CDs.

Figure S6

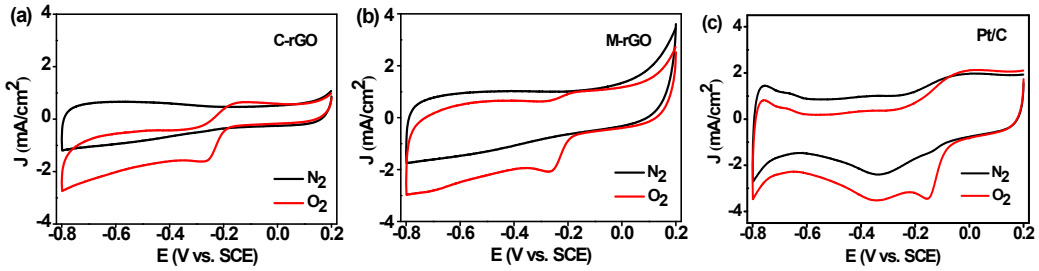

Figure S6 CV curves for the C-rGO (a), M-rGO, and Pt/C (c) in N_2-saturated and O_2-saturated 0.1 M KOH solutions at a scan rate of 10 mV s^{-1}

Figure S7

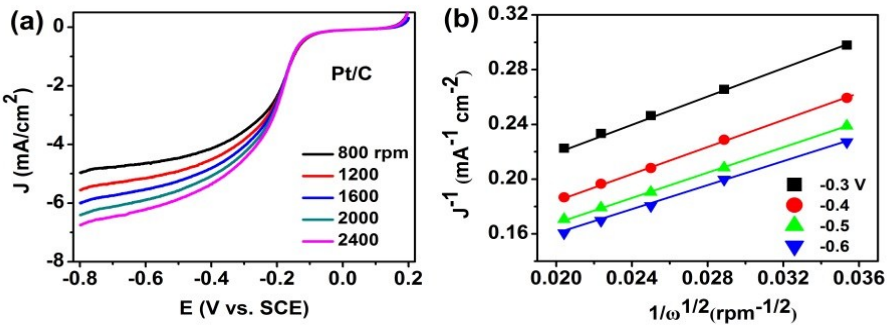

Figure S7 (a) RDE curves of the Pt/C at different rotation rates, (b) K-L plots at different potentials for the Pt/C.